Biomass Conversion and Biorefinery (2023) 13:7265–7285
https://doi.org/10.1007/s13399-022-02933-z

ORIGINAL ARTICLE

ANN-based sensorless adaptive temperature control system to improve methane yield in an anaerobic digester

Kundan Anand[1] · Alok Prakash Mittal[2] · Bhavnesh Kumar[2]

Received: 15 March 2022 / Revised: 3 June 2022 / Accepted: 7 June 2022 / Published online: 20 June 2022

Abstract

Constant methane yield from the biogas plants is necessary to achieve stable heat and power generation. From conventional biogas plants, a fluctuating methane yield is obtained due to variation in operating conditions. In this paper, an inferential control for constant methane yield by regulating the digester temperature is proposed. The optimal operating temperature of the digester is determined using artificial neural network (ANN). It considers variations in total volatile solids and hydraulic retention period to get constant methane yield. After training the proposed ANN, achieved MSE is 0.0003522, RMSE is 0.01876, and R^2 of 1 for training, validation, and testing. A proportional-integral-derivative controller tuned by bacterial foraging-particle swarm optimization along with a derivative filter has been used in the temperature control loop. In addition, the temperature sensor is replaced by a temperature estimator in the control loop. The performance of the proposed control scheme has been examined for various realistic operating conditions using MATLAB software.

Keywords ANFIS · ANN · Biogas plant · Inferential control · Sensorless control · Temperature control

1 Introduction

Anaerobic digestion (AD) is one of the key technology adopted by the growing agro-industries to effectively manage the waste produced [1, 2]. These industries produce a huge quantity of effluents having high organic content. Proper treatment of these effluents by AD plants not only generates bioenergy from it, but also reduces their adverse impact on the environment. Along with organic manure and fertilizer, methane-rich biogas is produced as an end product by these AD plants. Biogas has methane as the major component (55–75%) [3]. However, the quantity and quality of biogas depend on temperature, effective volume, volatile solid concentration, and methanogens [3–5].

Continuous online monitoring of substrate composition and coordinated control of AD are essential for high methane yield [6, 7]. However, the designing of a coordinated control system for a complex process like AD is a challenging task. The reasons behind the complexity are the uncertainties, non-linear behavior, and large time delays [8]. In addition, methane production using the AD method is a very slow process [9, 10]. Thus, methane production is hard to control using conventional control methods employing traditional sensors because of large and dynamic time delays [8, 11]. Intelligent soft sensors can aid control schemes and monitoring schemes in handling these issues.

Intelligent sensors including Adaptive Neural Fuzzy Inference System (ANFIS), Artificial Neural Network (ANN), Unscented Kalman Filter (UKF), and Response Surface Methodology (RSM) have been developed for variety of purposes [12]. Some of the application areas and the purposes for intelligent sensors are summarized in Table 1.

Highlights
- Controlled methane production by varying the temperature.
- Implemented temperature control of digester using ANN.
- Developed sensorless control for digester temperature.
- Applied bacterial foraging-PSO algorithm to tune PIDF controller.

✉ Bhavnesh Kumar
kumar_bhavnesh@nsut.ac.in

Kundan Anand
kundan.ee19@nsut.ac.in

Alok Prakash Mittal
alok@nsut.ac.in

[1] Electrical Engineering Department, Netaji Subhas University of Technology, Delhi, India 110078

[2] Instrumentation and Control Engineering Department, Netaji Subhas University of Technology, Delhi, India 110078

Table 1 An overview of the applications of soft-sensors

Area of application	Techniques	Purpose	Remarks	Reference
Distillation Process	ANN	Prediction of ethanol yield in the distillation process using temperature data	ANN achieved the mean square error of 0.2596	[8]
Small-scale production of biogas was undertaken using mushroom compost	ANFIS, ANN	Prediction of biogas yield using temperature, carbon to nitrogen ratio, and hydraulic retention period data	Performance of ANFIS was better than ANN	[13]
Full-scale (1200 L) batch reactor under 14 mesophilic conditions	ANFIS	Prediction and optimization of biogas production from cow 12 manure with maize straw under various total solid content (TS), carbon to nitrogen (C/N) 13 ratio, and stirring intensity	Eight percent increase in biogas yield while operating digester at conditions suggested by ANFIS	[14]
Estimation of biogas yields	RSM, ANFIS	Estimation of biogas yields produced from the combination of waste materials	From performance parameters, it was concluded that the predictive ability of ANFIS is better than RSM	[15]
Two-phase anaerobic digestion model	ANFIS	Prediction of biogas yield from anaerobic digestion of solid waste obtained from the leather industry	ANFIS achieved the mean-square error of 0.00049	[16]
Modular biodigester	ANFIS, ANN, RSM	Prediction of biogas production by using poultry wastes and cow dung	Performance of RSM was better than ANFIS and ANN	[17]
Control of bioprocess	UKF	Real-time monitoring of substrate and biomass for efficient control of bioprocesses	UKF was able to predict highly accurate values of the biomass and operating conditions of the digester even with 10% noise	[18]
Nicotiana tabacum L. oil biodiesel production	ANN, ANFIS	Used ANFIS and ANN for the modeling of tobacco seed oil methyl ester (TSOME) yield from underutilized tobacco seeds	The performance of ANFIS was better than ANN	[19]
Usage of graphene oxide (GO) nanoparticles with orange peel biodiesel for IC engine	ANN	Predicting the behavior of different injection pressure characteristics	RMSE value for the BTE, brake-specific energy consumption (BSEC),CO, HC, NOx, and smoke is obtained to be 0.036, 0.0216, 0.044, 0.041, 0.0446, and 0.0435, respectively	[20]
Prediction models for waste sunflower oil biodiesel	RSM-PSO	Correlate the optimal yield and trans-esterification variables for methylic biodiesel production	From performance parameters, it was concluded that the PSO model was better than the RSM model	[21]
Fermentation processes	Recurrent neural network (RNN)	Prediction of biomass concentration online	Achieved an accuracy of ± 11%	[22]

In most of the reported literature, it is proposed to estimate, predict, or forecast the methane yield rather than to control it. However, the control of crucial parameters influencing the methane yield is essential to control methane yield. It is a well-known fact that the methane yield is highly dependent on the concentration of volatile solids, hydraulic retention period, and operating temperatures [23]. Furthermore, among various operating parameters, the influent total volatile solids (VS), digester operating temperature (T_d), and hydraulic retention period (B) are independent parameters that may affect the methane yield [13].

Control over the concentration of volatile solids and hydraulic retention period is very complex as compared to the control of digester temperature [24]. Therefore, the desired methane yield may be achieved by operating the digester at a temperature value determined based on the concentration of volatile solids and hydraulic retention period. Therefore, an inferential control strategy is presented in this paper to obtain desired methane yield. The digester is operated at optimum temperature value according to the required methane yield, volatile solids, and hydraulic retention period determined by ANN.

The temperature of the digester is varied using a flow valve control method with a proportional integral derivative controller with a derivative filter (PIDF). The gains of the PIDF controller are optimized by the bacterial foraging-particle swarm optimization (BF-PSO) technique. The complete schematic of the conventional AD process and proposed inferential control strategy for methane yield production is presented in Fig. 1. Furthermore, in the proposed inferential control strategy, a temperature sensorless method is used to control the temperature of the digester.

In this paper, the research methodology is presented in Section 2, and the obtained results from the proposed control strategy are presented in Section 3. The conclusion and future scope are presented in Section 4.

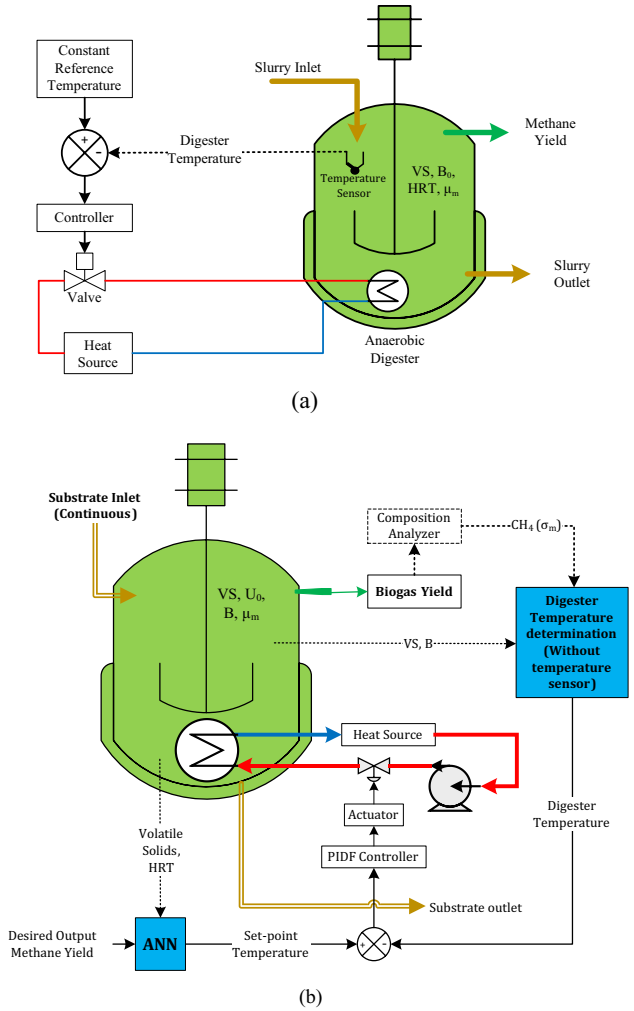

Fig. 1 Schematic of AD process control strategy: **a** conventional [13] and **b** inferential

2 Research methodology

2.1 Anaerobic digester

The anaerobic digester model is modeled in MATLAB/Simulink 2021a to conduct the analysis [25–27]. The reference values of all the parameters used are presented in Table 2. The methane production rate (σ) can be obtained by following the simplified AD model [26].

$$\sigma = \frac{U_0 \times VS}{B}\left\{1 - \frac{C}{(\mu_m \times B) - 1 + C}\right\} \quad (1)$$

Here, U_0 is the ultimate methane yield ($L(CH_4)/g$ (VS)), *VS* is influent total volatile solids (g (VS)/L(slurry)), *B* is the hydraulic retention period (days), μ_m is the growth rate of methanogens, and *C* is the kinetic constant. The growth rate of methanogens depends on the operating temperature (T_d) (°C) of the digester which can be calculated by Eq. (2) [28]:

$$\mu_m = \left(0.013 \times T_d\right) - 0.129 \quad (2)$$

For the production of the required quantity of methane (V_{CH4}) (m^3), the effective volume of the digester (V_r) (m^3) can be calculated by Eq. (3) [26]:

$$V_r = \frac{V_{CH4}}{\sigma} \quad (3)$$

whereas, the required flow rate of influent slurry (F_r) (m^3/h) can be determined by the Eq. (4) [26]:

$$F_r = \frac{V_r}{24 \times B} \quad (4)$$

Table 2 Reference values for the parameters of the AD model

Parameter	Value (in literature)	Reference	Variation considered in values
Methane production (σ) (m^3)	––	––	––
Required biogas yield (Nm^3/day)	5000	––	––
Ultimate methane yield (U_0)(L (CH_4)/g (VS))	0.32	[25–27]	––
Influent total volatile solids (VS) (g (VS)/L (slurry))*	60	[25–27]	40–70
Hydraulic retention period (B) (in days)*	20	––	1–5
Kinetic constant parameter (C)	0.9	[25–27]	––
Digester operating temperature (T_d) (in °C)*	35	[25–27]	25–65

*Parameters considered for variation

2.2 Data preparation

A data set of 525 values of methane yield was generated. The data set was generated by considering the variations in volatile solids (VS), digester operating temperature (T_d), and hydraulic retention period (B). The dataset has been created by randomly generating the values of the considered parameters in ranges mentioned in Table 2. The AD model used to generate the dataset is presented by Eq. 1.

2.3 Design of ANFIS-based soft-sensor

ANFIS is an amalgamation of ANN and fuzzy logic with the Takagi–Sugeno inference system. The advantages and potential of both systems are presented in a single framework. Its inference system corresponds to a set of fuzzy if–then rules, with the learning and predictive ability of nonlinear functions [29–31]. In this work, ANFIS is used to determine the temperature at which the digester must be operated to obtain specific methane yield according to total volatile solids (VS) and hydraulic retention period (B). There are three inputs to ANFIS and one output, i.e., desired methane yield, hydraulic retention period, total volatile solids, and temperature, respectively (Fig. 2). The structure of the proposed ANFIS model is presented in Fig. 3. The root mean square error (RMSE) is minimized while training ANFIS and can be expressed as:

$$\mathrm{RMSE} = \sqrt{\frac{\sum_{z=1}^{z_n} (x_z - \hat{x}_z)^2}{z_n}} \tag{5}$$

here, z_n is the number of data points, x_z is the actual observation time series, and $\hat{x}_z$ is the estimated time series data.

2.3.1 ANFIS training

A data set of 525 values generated using Eq. 1 has been used to train ANFIS for determining the temperature at which the digester must be operated to obtain the required methane yield based on total volatile solids and hydraulic retention time. The optimization method used while training ANFIS is an amalgamation of the backpropagation and least square method [32]. The backpropagation method is used to train input membership functions, whereas the least square method is used to train the output membership functions of ANFIS. The trained membership functions of ANFIS are presented in Fig. 4. Five bell-shaped membership functions are considered for each input. All

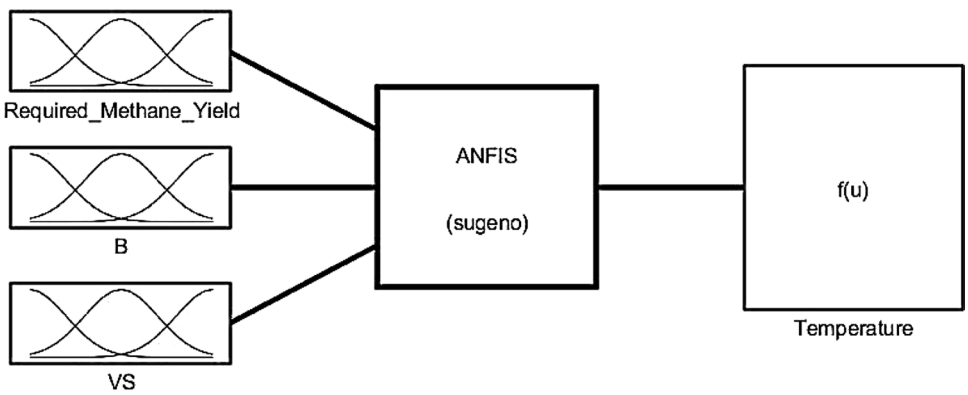

Fig. 2 Architecture of ANFIS model

membership functions are satisfying the minimum 50% overlap condition to avoid indecisive behavior from fuzzy logic.

The trained ruleset is presented by the surface plot in Fig. 5. The surface plot represents the variation in temperature with variation in required methane yield, VS, and B.

Response of ANFIS training for minimum root mean square error (RMSE) equal to 0.01904 is shown in Fig. 6.

In Fig. 7, the trained output obtained against the training data is presented. From the response, it can be observed that the trained ANFIS output is almost mapping with the training data. No considerable deviation in ANFIS output

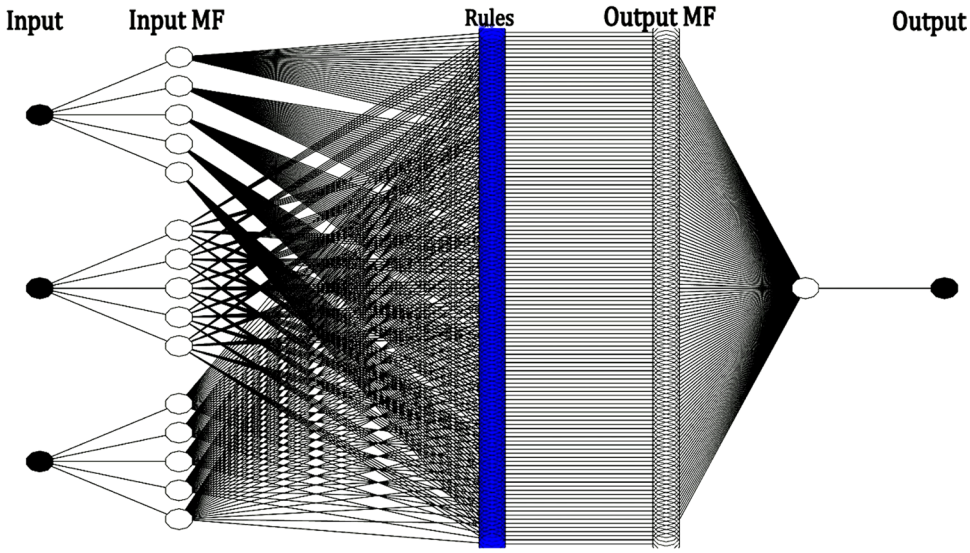

Fig. 3 Structure of ANFIS model with 42 fuzzy rules and 342 nodes

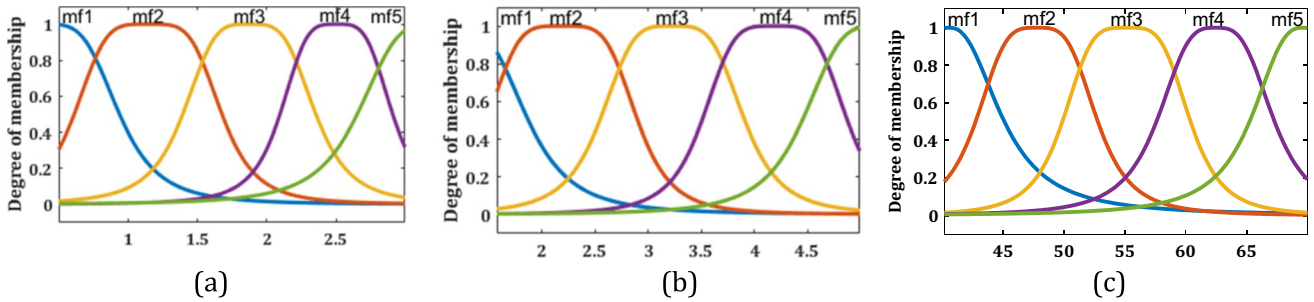

Fig. 4 Trained ANFIS membership function for **a** required methane yield, **b** hydraulic retention period, and **c** total volatile solids

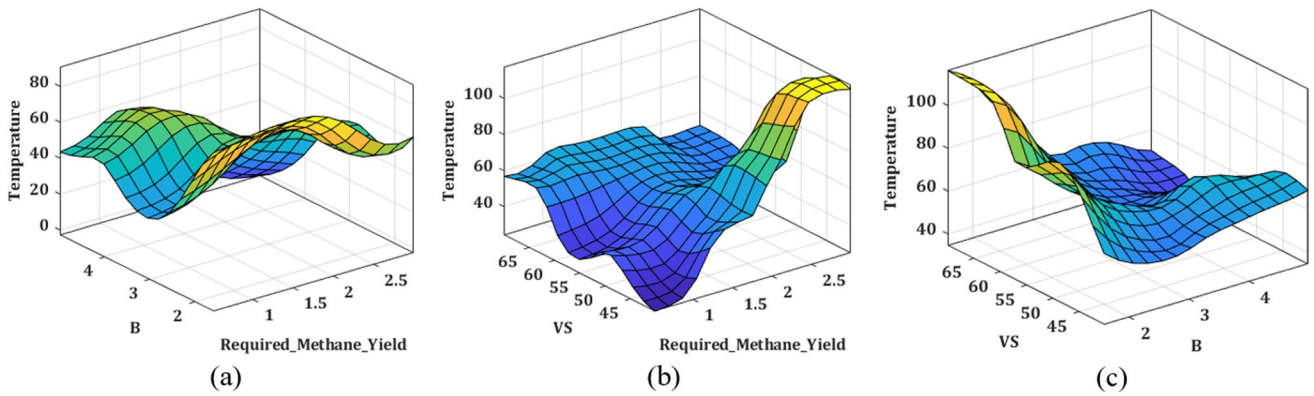

Fig. 5 Surface plot for variation in temperature with variation in **a** required methane yield and B, **b** required methane yield and VS, and **c** VS and B

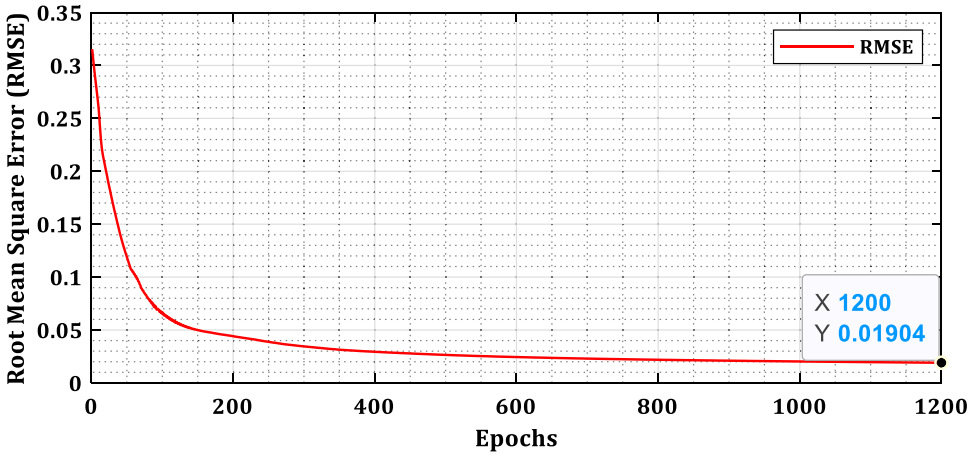

Fig. 6 Training error for ANFIS

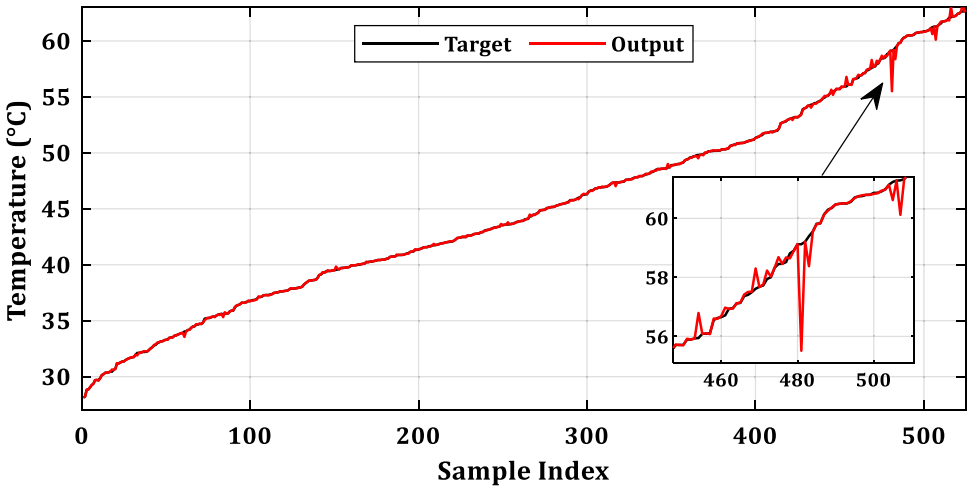

Fig. 7 ANFIS trained output vs ANFIS training data

from actual data is observed. To maintain accuracy, a large sample size is taken for the training purpose. In Fig. 8, the regression plot of ANFIS training is presented. The achieved R^2 for training, validation, testing, and overall are 1, 0.99961, 0.99742, and 0.99950, respectively.

2.4 Design of ANN-based soft-sensor

A collection of connected trained neurons that act as an artificial brain is called artificial neural network (ANN). ANN has the learning and predictive ability of nonlinear functions. ANN consists of three layers, i.e., input layer, hidden layer, and output layer [13, 33]. In the present work, there are three inputs in the input layer, i.e., required methane yield, hydraulic retention period (B), and total volatile solids (VS). The number of neurons in the hidden layer has been selected based on the dimension of input and the number of training pairs. The equation presented below has been used to calculate the adequate number of neurons in the hidden layer (H_n).

$$H_n = C_n \times \sqrt{\frac{N_d}{I_m \times \log N_d}} \tag{6}$$

here, C_n is a constant, N_d is the number of data pairs, and I_m is the dimension of input. When the ratio of N_d and I_m is greater than 30, the value of C is either 1 or 2 [34, 35]. Here, in the hidden layer, there are twenty neurons.

The transfer function of the hidden layer is of the tan-sigmoidal (TANSIG) type for proper adaptability. The output layer has one neuron and has a pure linear (PURELIN) transfer function. The type of network is the feed-forward backdrop. The network uses the most popular Levenberg–Marquardt backpropagation algorithm for training purposes [13, 36]. Moreover, gradient descent with momentum weight and bias learning function has been used. An error is generated by comparing the model output with the desired output and sent back to the hidden and input layer for training. The training ends when the error is reduced to a user-defined value, i.e., zero. From the dataset of 525 values, 75% of these were kept for training and the remaining for validation and

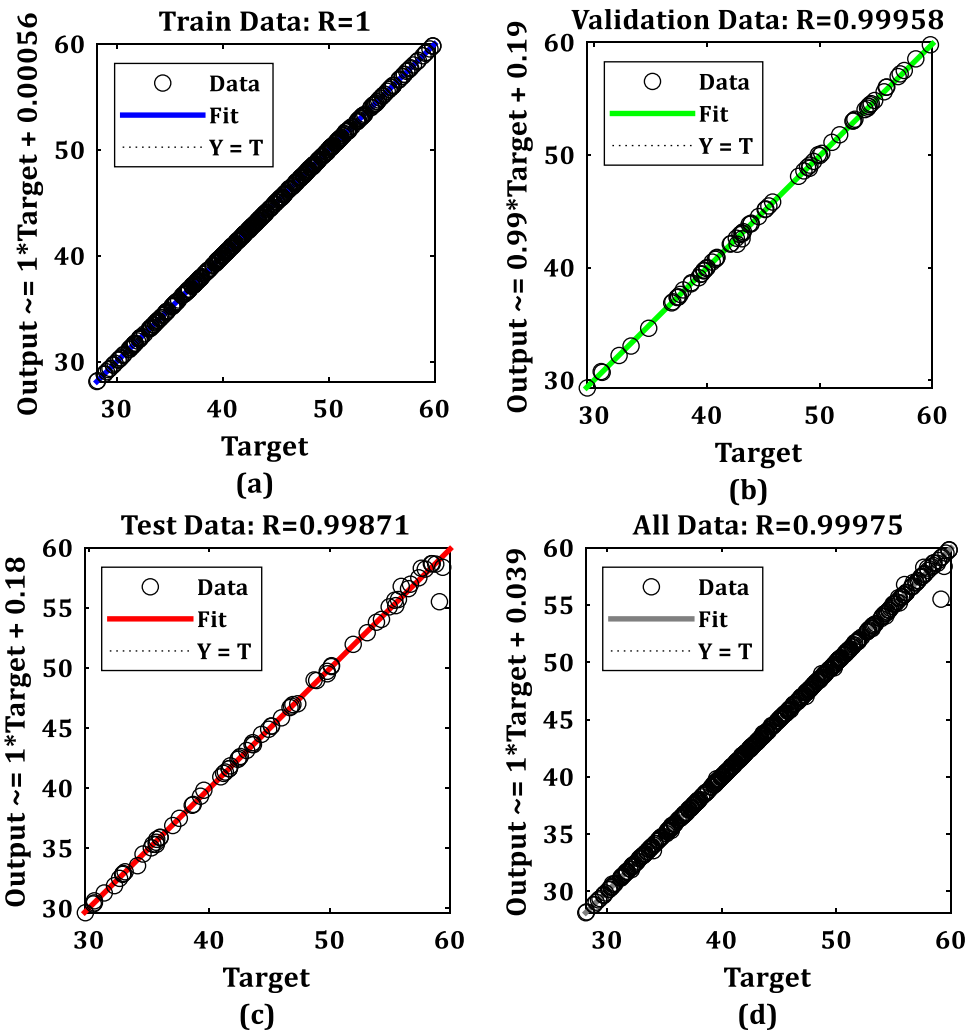

Fig. 8 Regression plot for ANFIS **a** training, **b** validation, **c** testing, and **d** overall

testing. The performance of the designed network is judged based on the mean square error (MSE) given in Eq. (7).

$$\mathrm{MSE} = \frac{1}{z_n}\sum_{z=1}^{z_n}(y_z - \hat{y}_z)^2 \tag{7}$$

2.4.1 Post training data of ANN

The designed ANN is presented in Fig. 9. The training of ANN has been conducted with 20, 15, and 10 neurons. Best validation performance for mean square error (MSE) of 3.5221×10^{-04} is obtained at epoch 906 with 20 neurons (Table 3) (Fig. 10). The regression plot obtained after training shows a perfect fit ($R = 1$) of data in the case of training, validation, testing, and overall with 20 neurons (Fig. 11).

2.5 Temperature control system

AD plant is operated on the temperatures decided by ANFIS and ANN separately. The temperature of the digester is regulated by the PIDF controller-based flow valve control method. A smith predictor has also been used to increase the stability and improve the performance of the temperature control

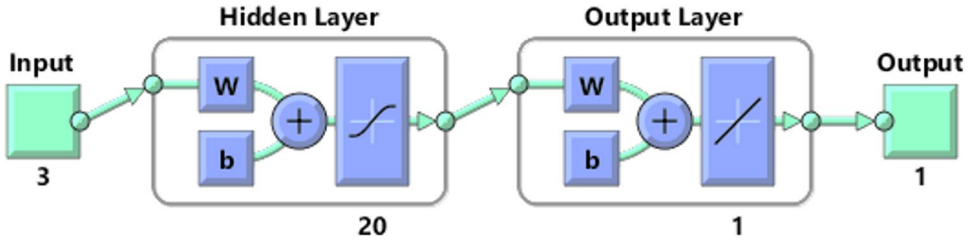

Fig. 9 The architecture of the proposed ANN

Table 3 Comparison table for variation in the number of neurons in the hidden layer

Number of neurons	Mean square error (MSE)	Epochs	Best validation at epoch	Validation failed at	Training regression	Validation regression	Test regression	Overall regression
20	0.00035221	1000	906	–-	1	1	1	1
15	0.0003998	1500	1264	1464	1	1	0.99999	1
10	0.0087679	1200	1998	–-	1	0.99998	0.99999	0.99999

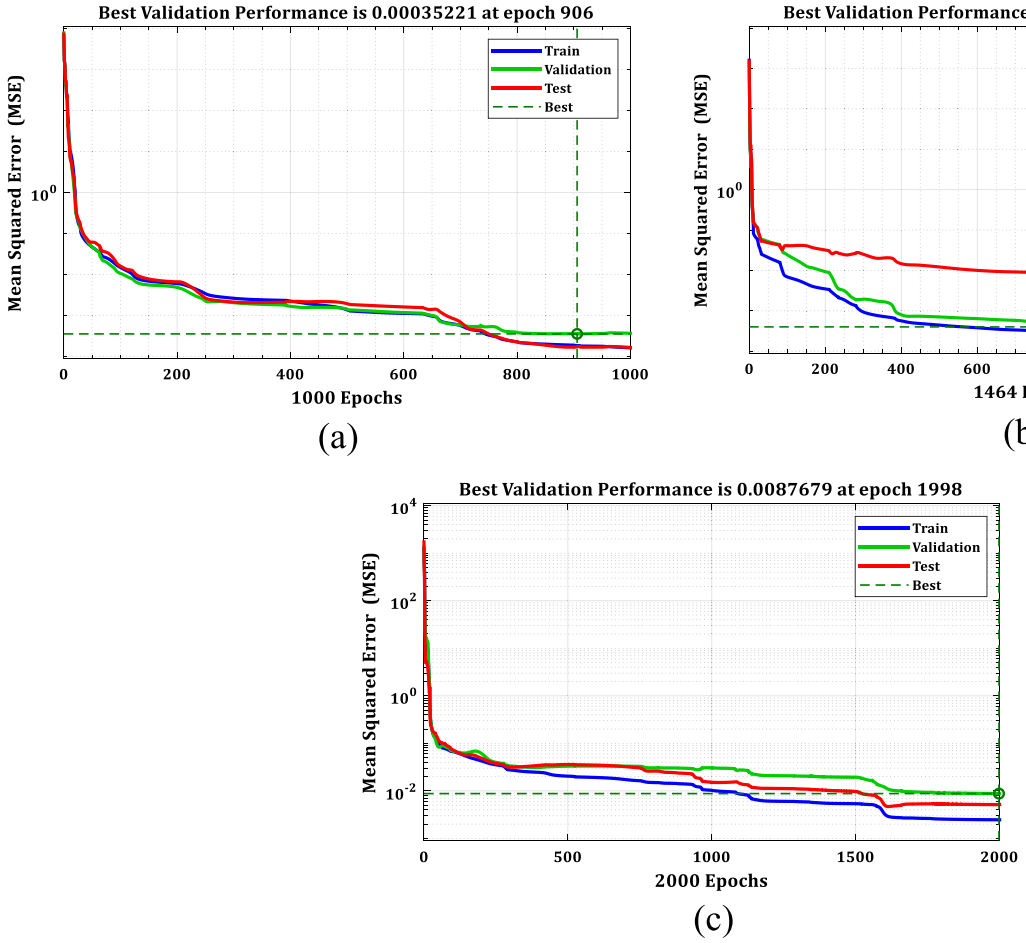

Fig. 10 Performance of ANN in terms of mean squared error with **a** 20 neurons, **b** 15 neurons, and **c** 10 neurons

system. The parameters of the PID controller (i.e., K_P, K_I, and K_D) have been estimated by the bacterial foraging-particle swarm optimization (BF-PSO) technique, by minimizing integral time absolute error (ITAE). ITAE has been used due to its advantage of integral time factor over integral square error (ISE) and integral absolute error (IAE). The ITAE produces minimum overshoot with low rise time and settling time [37]. The heating coil, temperature sensor, and actuator have first order plus time-delay (FOPTD) transfer functions. The schematic of the conventional temperature control strategy and the proposed control strategy is presented in Fig. 12. Furthermore, in the proposed inferential control strategy, instead of using a temperature sensor for temperature control of the digester, the digester temperature is calculated by the following equation:

$$\frac{\frac{U_0 \times VS \times C}{(U_0 \times VS) - (B \times \sigma)} + 1 - C}{B} + 0.129 = T_d \quad (8)$$

2.5.1 PID controller with derivative filter (PIDF)

It has been reported in the literature that the conventional PID controllers can introduce undesirable vibrations in the actuator

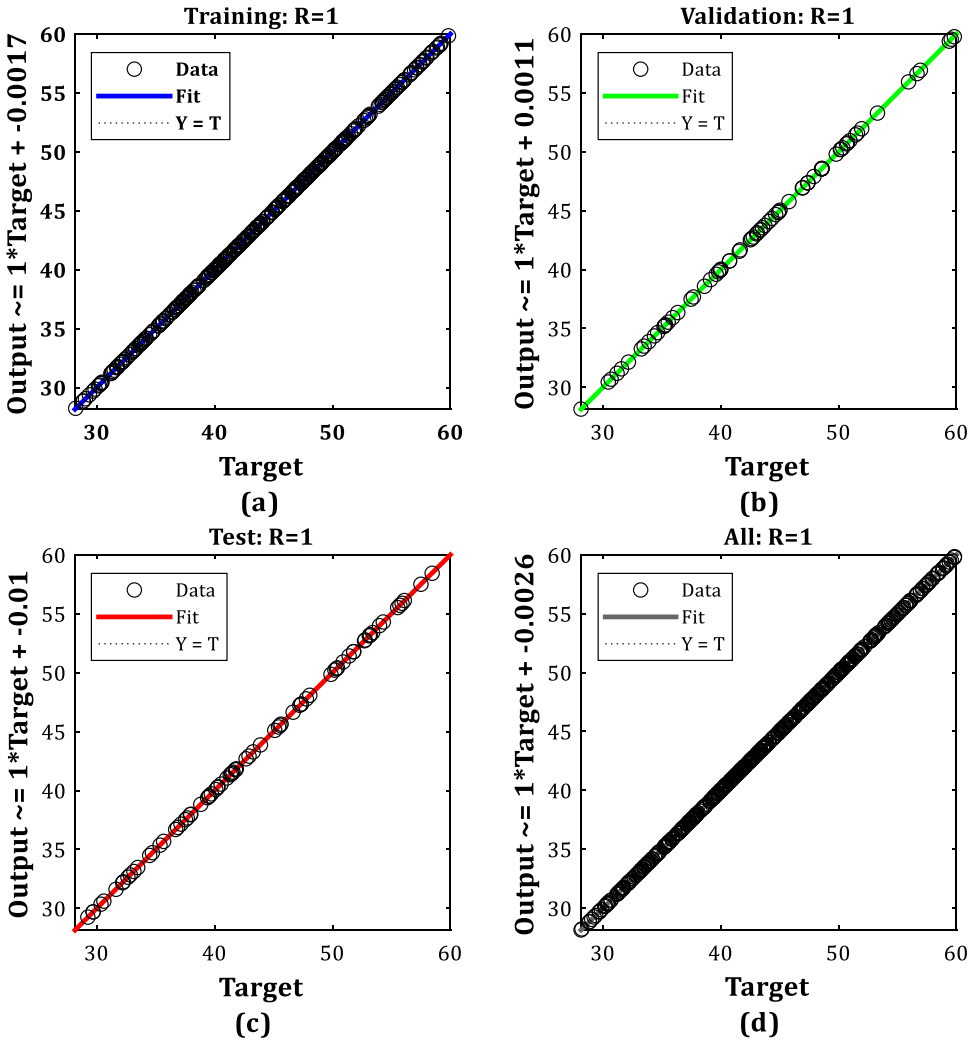

Fig. 11 Regression plot for 20 neurons: **a** training, **b** validation, **c** testing, and **d** overall

and valve under dynamic conditions [38]. Therefore, to overcome the oscillatory response, a filter is added in series with the derivative term used. It acts as a low pass filter that restricts the high-frequency derivative gains and noises. The PID controller with a derivative filter can be designed using Eqs. (9) and (10). The structure of the PIDF controller is presented in Fig. 13.

$$U(s) = K_P \times E(s) + K_i \times \frac{E(s)}{s} + K_d \times \hat{E}(s) \times \frac{K_n s}{s + K_n} \quad (9)$$

$$K_n = \frac{2 \times K_P}{K_d} \quad (10)$$

2.5.2 Bacterial foraging-particle swarm optimization (BF-PSO)

The BF-PSO is an amalgamation of two optimization algorithms, i.e., particle swarm optimization (PSO) and bacterial foraging (BF). Hybridization overcomes the drawback of bacterial foraging and particle swarm optimization (PSO), i.e., delay in reaching optimal solutions due to extreme random search directions and entanglement in local solutions, respectively. The BF-PSO enhances the convergence speed and eliminates local solution entanglement [39, 40]. The flowchart for BF-PSO algorithm is given below in Fig. 14:

Responses for achieving desired fitness value for different optimization algorithms are shown in Fig. 11. From Fig. 15, it is evident that the integral time absolute error (ITAE) parameter is low for the bacterial foraging-particle swarm optimization algorithm (BF-PSO) compared to the genetic optimization algorithm (GA) and particle swarm optimization (PSO). The elapsed time during training for BF-PSO, PSO, and GA is 12.15 min, 13.4 min, and 15.5 min, respectively, for 100 iterations in MATLAB Simulink 2021a. Furthermore, from Fig. 15, it can be observed that the optimum result is obtained at the 59th iteration in the case of the BF-PSO algorithm.

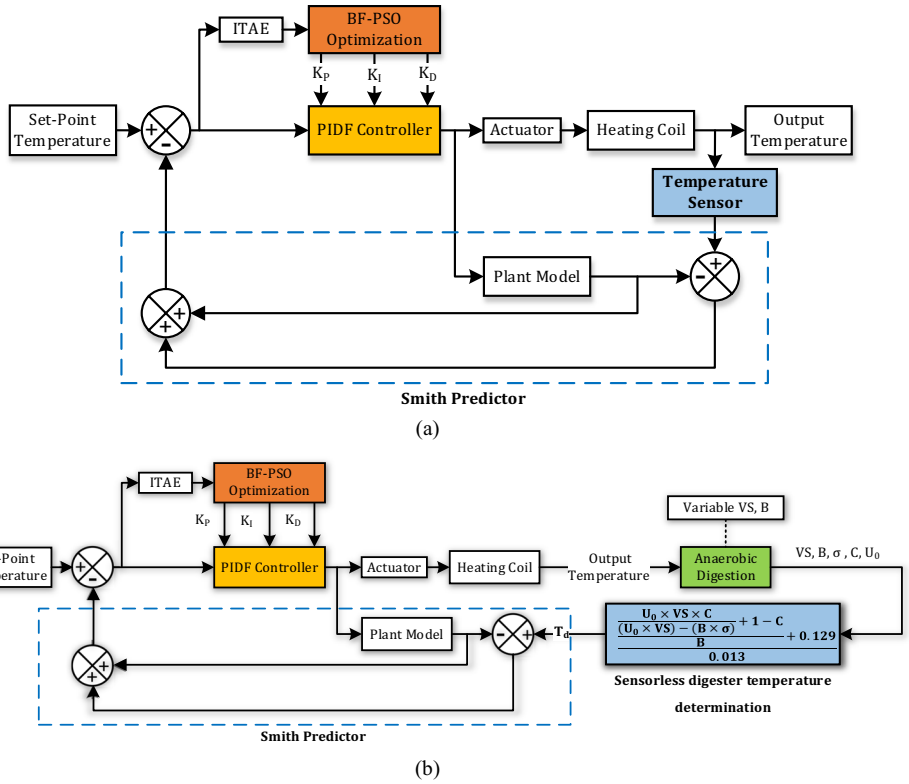

Fig. 12 Diagram for **a** conventional temperature control strategy with smith predictor. **b** Proposed "temperature sensorless" temperature control strategy with smith predictor

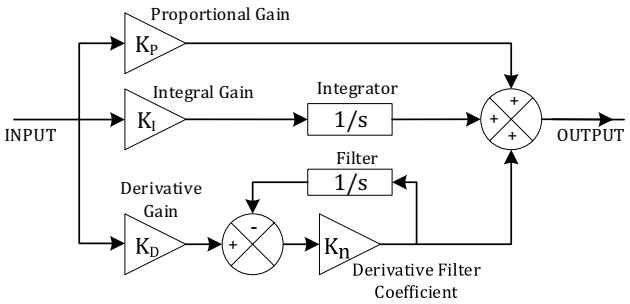

Fig. 13 Structure of PID controller with derivative filter (PIDF)

2.6 Inferential control of methane yield

An inferential control strategy to obtain constant methane yield under variable solid concentration and hydraulic retention period is proposed in this research. Here, the desired methane yield is achieved by operating the digester at a temperature value determined based on the concentration of volatile solids and hydraulic retention period. The digester temperature is controlled by using a flow valve control. A PIDF controller is used to regulate the flow of hot fluid to control the temperature of the digester. The gains of the

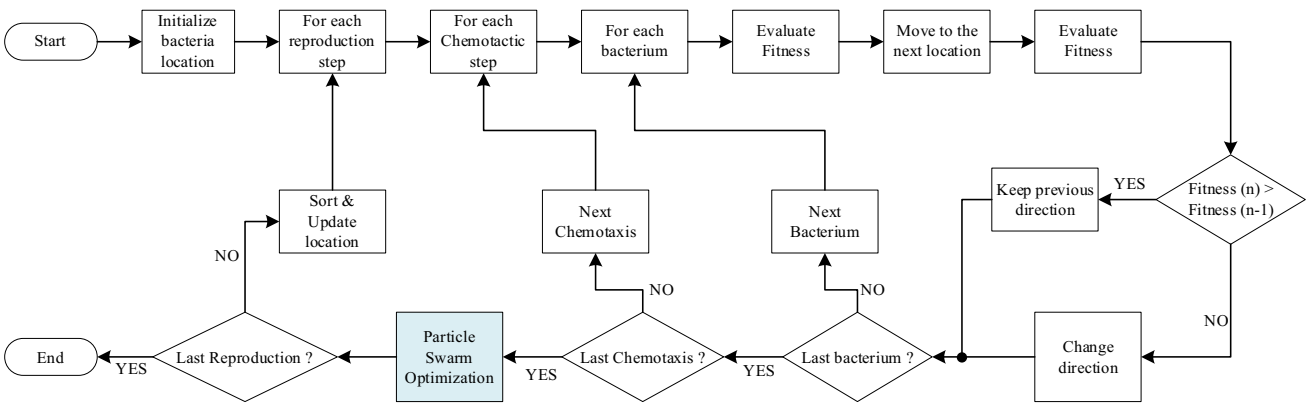

Fig. 14 Flowchart for BF-PSO optimization algorithm

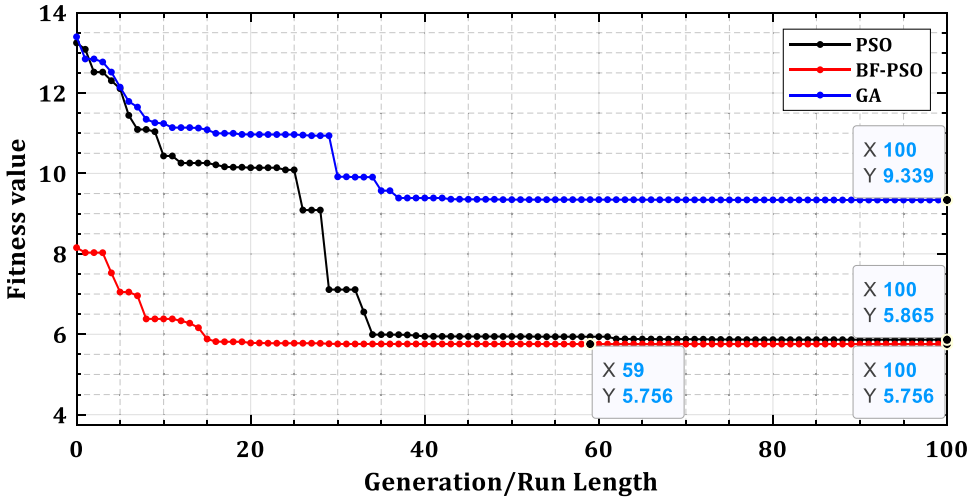

Fig. 15 Graph for fitness value

PIDF controller are obtained by the bacterial foraging-particle swarm optimization (BF-PSO) technique. Furthermore, in the proposed inferential control strategy, instead of using a temperature sensor for temperature control of the digester, the digester temperature is calculated by the following equation. The proposed inferential control strategy for methane yield is presented in Fig. 16.

3 Results and discussions

The system under consideration is simulated for different operating conditions. The key results obtained are as follows:

3.1 ANFIS and ANN accuracy

From Fig. 17, it can be observed that the error in trained output values is very less in ANN with 20 neurons, whereas the error in trained output values is higher in ANFIS compared to ANN. Furthermore, a comparison between training performances of ANFIS and ANN is presented in Table 4. From Fig. 17 and Table 4, it can be said that the accuracy of ANN is higher compared to ANFIS.

3.2 Sensitivity analysis of AD plant

The effect of volatile solids (VS), hydraulic retention period (B), and digester operating temperature (T_d) on methane yield is analyzed by using a sensitivity analyzer application on the AD model simulated in MATLAB/Simulink 2021a. From Figs. 18, 19, and 20, it can be concluded that the maximum methane yield can be obtained at a thermophilic temperature of around 55 °C. Meanwhile, the hydraulic retention period (B) must be kept for around 4 days and the concentration of total volatile solids must be kept at around 60 g/L.

3.3 Methane yield during controlled temperature

Response of the AD plant obtained during variations in the concentration of volatile solids and hydraulic retention period is observed. The temperature of the digester is varied according to the reference temperature obtained from the proposed ANN. To examine the performance of the proposed control, the developed simulation model has been tested for the following realistic cases of variation in total volatile solids (VS) and hydraulic retention period (B) for a stabilized production of methane, i.e., 2.9 (m^3/m^3 of digester). The considered test conditions are presented in Fig. 21.

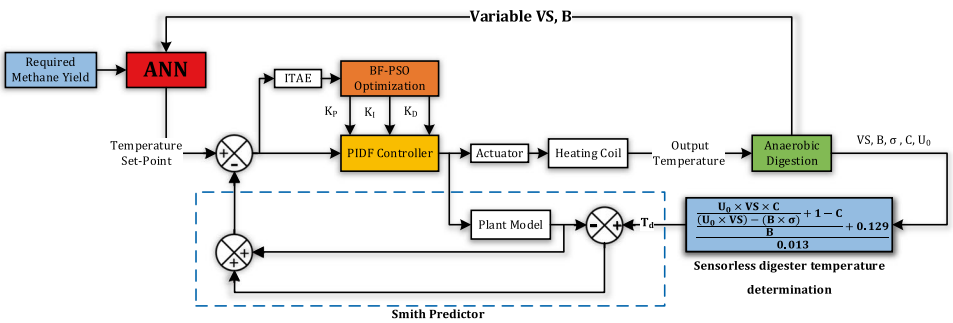

Fig. 16 Schematic of the proposed inferential control strategy for AD plant

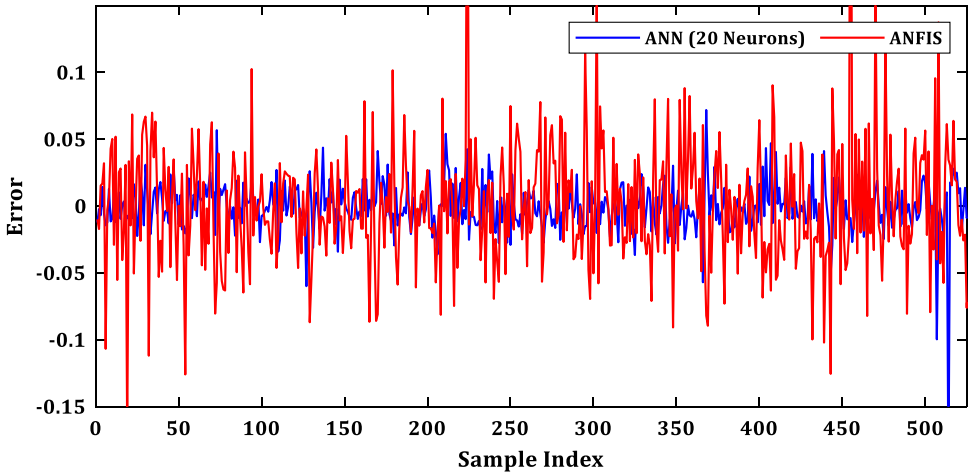

Fig. 17 Error in the trained output value of ANFIS and ANN

Table 4 Comparison between training performances of ANFIS and ANN

Sensor	Epochs	Nodes or neurons	MSE	RMSE	R^2 (training)	R^2 (validation)	R^2 (test)	R^2 (all data)
ANFIS	1200	342	0.00036252	0.01904	1	0.99961	0.99742	0.99950
ANN	1000	20	0.00035221	0.01876	1	1	1	1

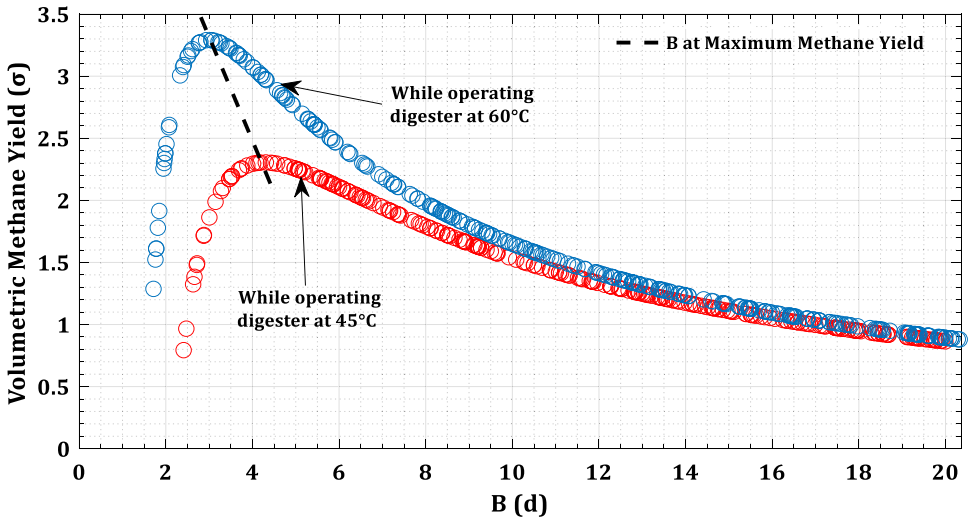

Fig. 18 Effect of variation in hydraulic retention period on methane yield while operating digester at 45 °C, 60 °C, and VS = 60

The study is divided into four cases on a time scale as follows:

Case-1: When VS = 58, B = 4, and required methane yield=2.9 (0-200h)
Case-2: When VS = 58, B = 3, and required methane yield=2.9 (200-400 h)
Case-3: When VS = 60, B = 4, and required methane yield=2.9 (600-800 h)
Case-4: When VS = 59, B = 3, and required methane yield=2.9 (1200-1400 h)

For the abovementioned cases, the variation in digester operating temperature, hot fluid flow rate, heat energy requirement, the growth rate of methanogens, digester effective volume, required feed flow rate, and volumetric methane yield has been studied.

Case-1: When VS = 58, B = 4, and required methane yield = 2.9 (0-200 h)

This case occurs during 0–200 h, 400–500 h, 800–1200 h, and 1400–1500 h. From Figs. 22 for this case, it can be observed that the reference temperature obtained by ANFIS and ANN is

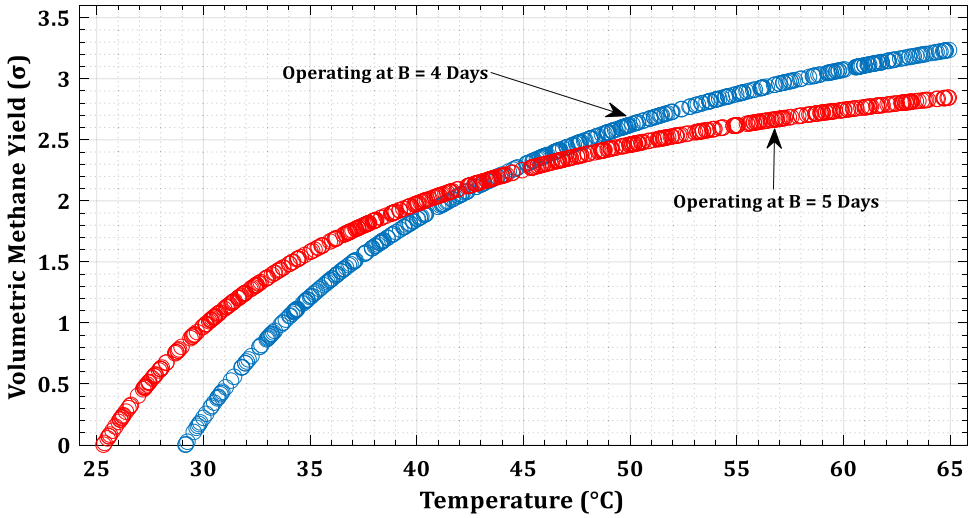

Fig. 19 Effect of variation in temperature on methane yield while operating digester at B = 4, 5 days, and VS = 60

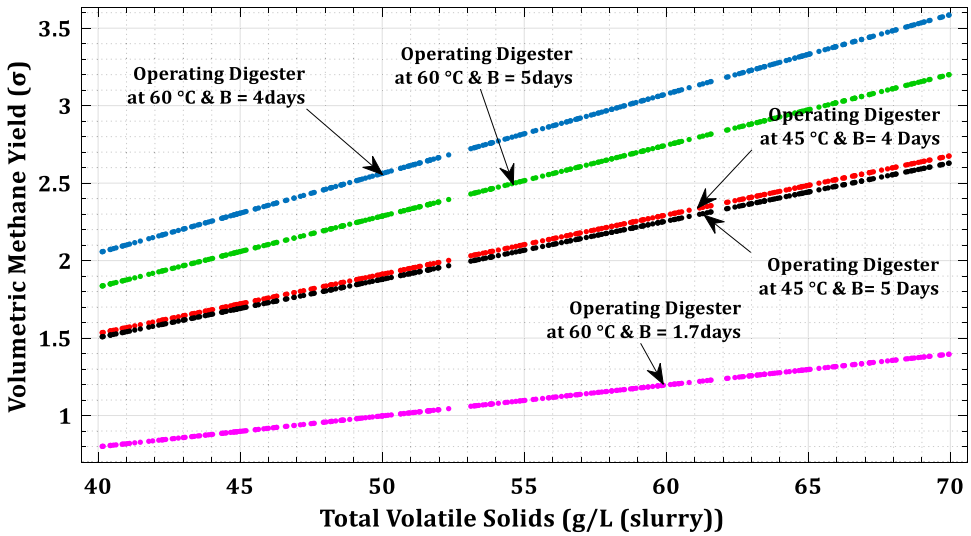

Fig. 20 Effect of variation in total volatile solids on methane yield while operating digester at temperature = 45 °C, 60 °C; B = 1.7, 4, 5 days

57.925 °C and 58.021 °C, respectively. If the AD is operated at the reference temperature obtained from ANFIS and ANN, then the desired methane yield of 2.9 (m^3/m^3 of digester) can be achieved when VS is 58 and B is 4. In constant temperature operation, the thermophilic set-point temperature 55 °C is considered. The obtained methane yield from the digester, in this case, is 2.897 m^3, 2.901 m^3, and 2.779 m^3 in the case of ANFIS, ANN, and constant temperature operation, respectively (Fig. 29). Deviation of methane yield from set-point can be observed in Fig. 30. It can be observed that the desired methane yield is achieved when the digester is operated at the reference temperature obtained from ANN. However, the methane yield obtained during the operation of the digester at the reference temperature obtained by ANFIS is less than a marginal difference. This marginal difference is due to lower reference temperature from ANFIS compared to ANN.

To maintain a higher temperature, higher hot fluid flow rate is required to meet higher heat energy demands [41]. In this case, the total heat energy required to maintain the reference temperature obtained by ANFIS, ANN, and constant temperature operation is 19.53 kJ/h, 19.62 kJ/h, and 16.89 kJ/h (Fig. 25), respectively. The hot fluid flow rate required to maintain the reference temperature obtained by ANFIS, ANN, and constant temperature operation is 0.12745 m^3/h, 0.12765 m^3/h, and 0.12101 m^3/h, respectively (Fig. 24). The higher the flow rate of hot fluid, the lower the rise time and settling time. From Fig. 23, it can be observed that the rise time to achieve the reference temperature obtained by ANN, ANFIS, and constant temperature operation is 2.915 h, 2.935 h, and 2.992 h, respectively. Whereas, the settling time is 4.953 h, 5.061 h, and 5.093 h, respectively. Peak overshoot is zero in all temperature control schemes. The digester operating temperature decides the growth rate of enzymes, feed rate, and digester effective volume.

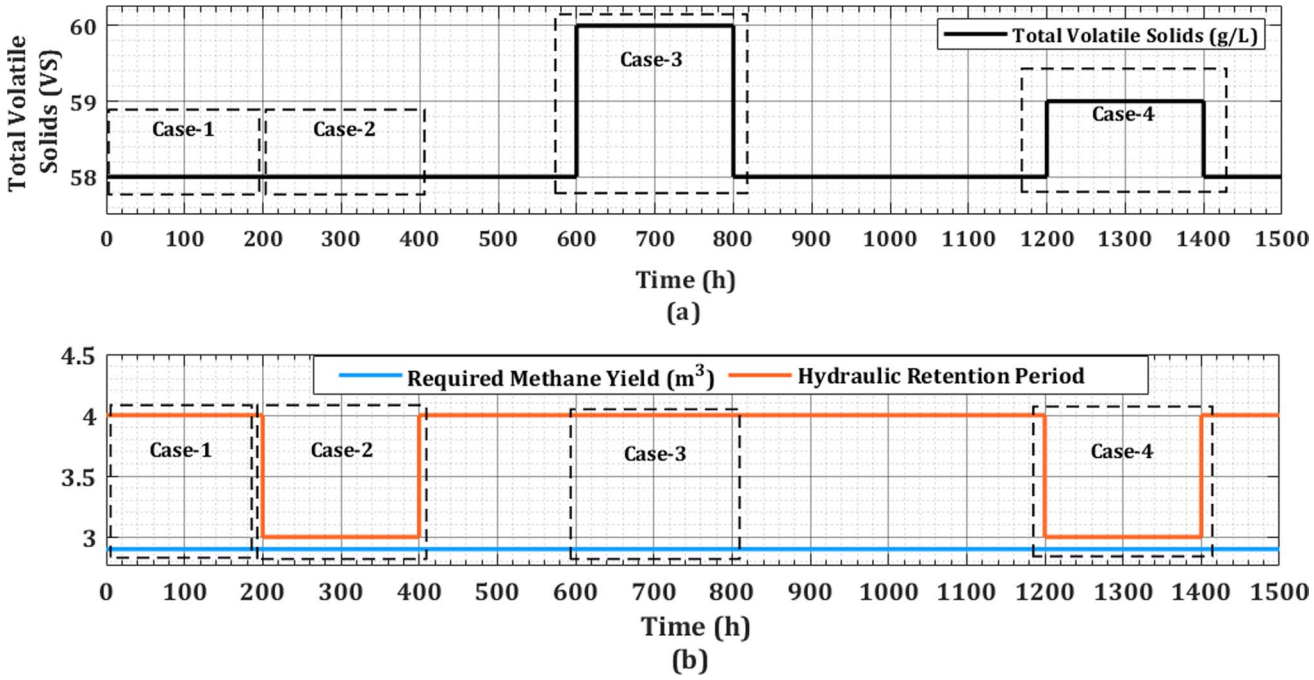

Fig. 21 Variation in **a** total volatile solids and **b** hydraulic retention period with the constant requirement of methane yield

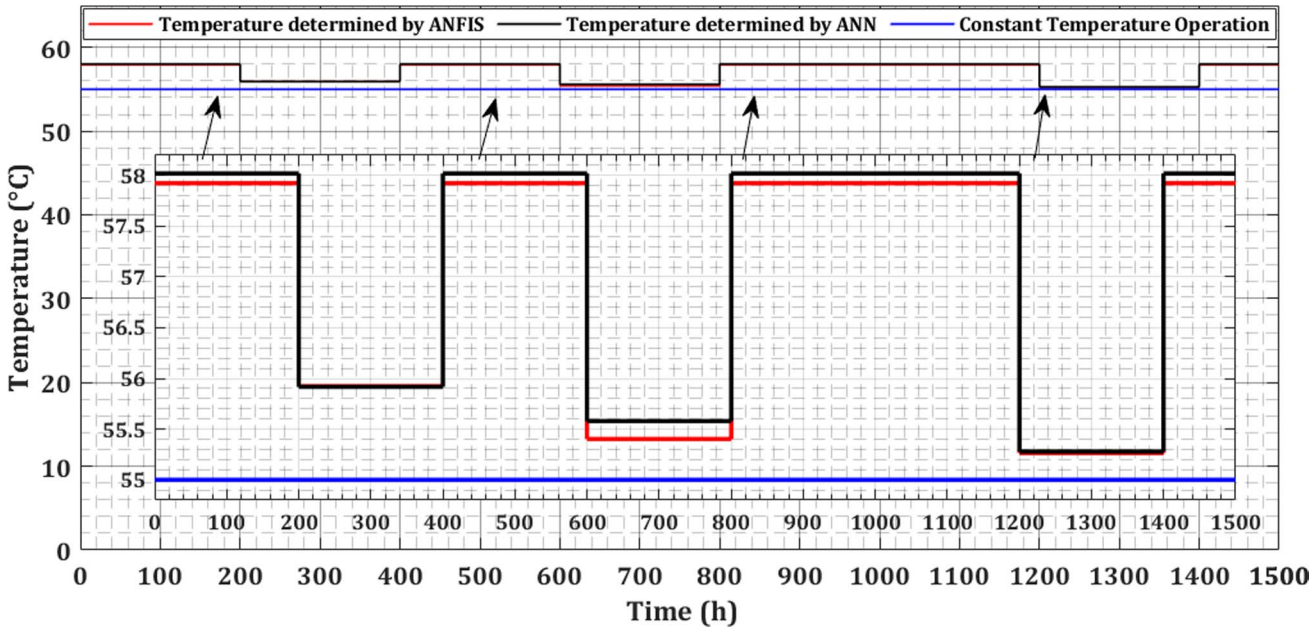

Fig. 22 Graph for temperature set-point produced from ANFIS and ANN compared with constant temperature operation

The growth rate of methanogens is 0.624, 0.626, and 0.586 when the reference temperature is obtained by ANN, ANFIS, and constant temperature operation, respectively (Fig. 26). The higher growth rate of methanogens represents a rapid conversion of substrate into methane. To produce the desired methane yield, the effective volume of the substrate inside the digester must be 28.995 m^3, 28.955 m^3, and 30.226 m^3 for the reference temperature which are obtained by ANN, ANFIS, and constant temperature operation, respectively (Fig. 27). To achieve the required effective volume of the substrate in the digester, a specific feed

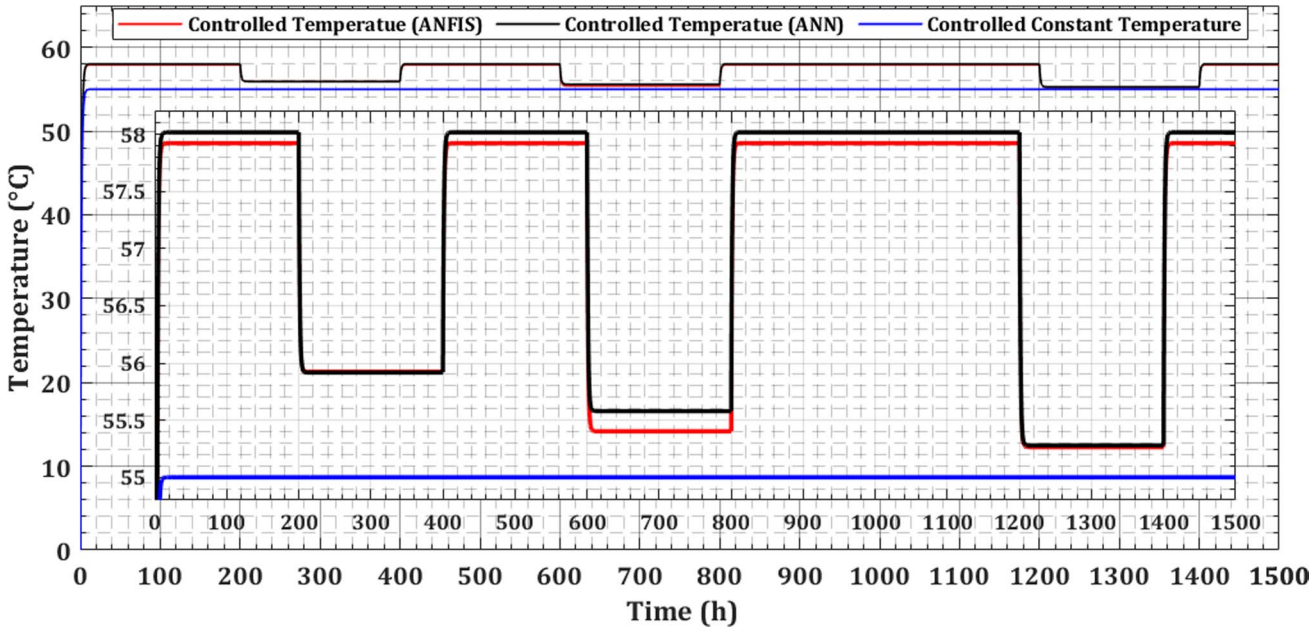

Fig. 23 Graph for controlled output temperature according to set-point temperature produced from ANFIS and ANN compared with constant temperature operation

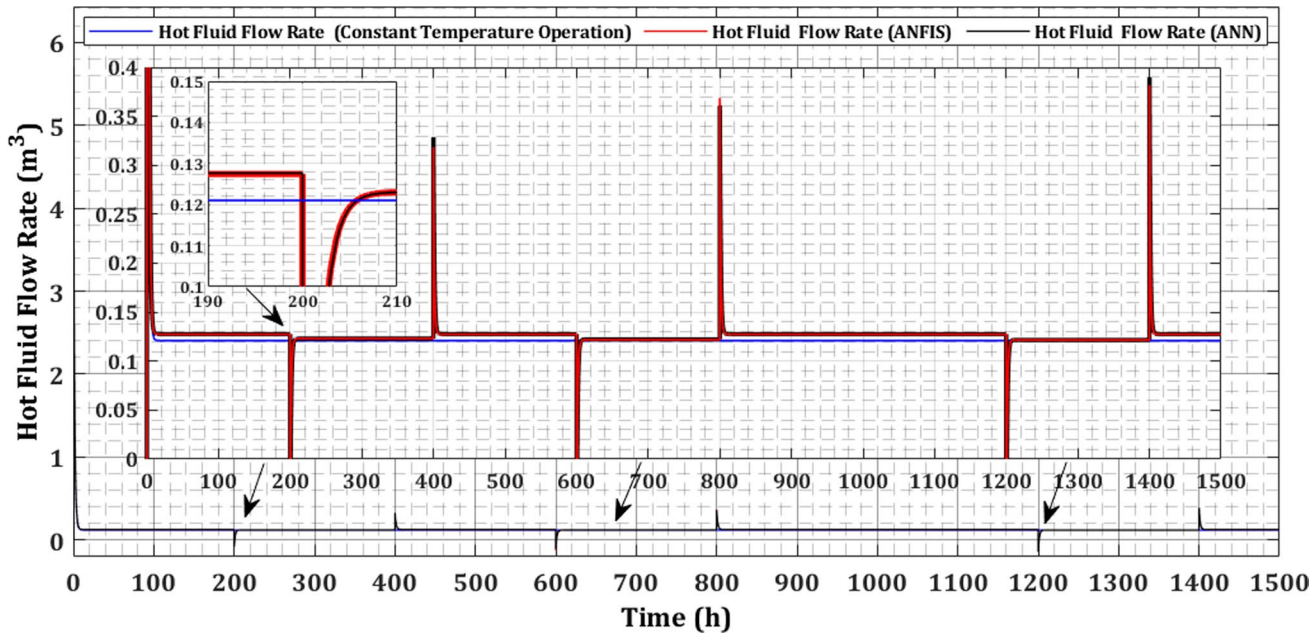

Fig. 24 Graph for variation in hot fluid flow rate due variation in temperature set-point produced from ANFIS and ANN compared with constant temperature operation

rate is required. The required feed rate in the digester is 0.0755 m^3/h, 0.0754 m^3/h, and 0.0785 m^3/h in the case for the reference temperature which are obtained by ANN, ANFIS, and constant temperature operation, respectively (Fig. 28).

Case-2: When VS = 58, B = 3, and required methane yield = 2.9 (200-400 h)

For this case, the temperature set-point determined by ANFIS is 55.92 °C whereas the temperature set-point determined by ANN is 55.91 °C (Fig. 22). From Fig. 23, it

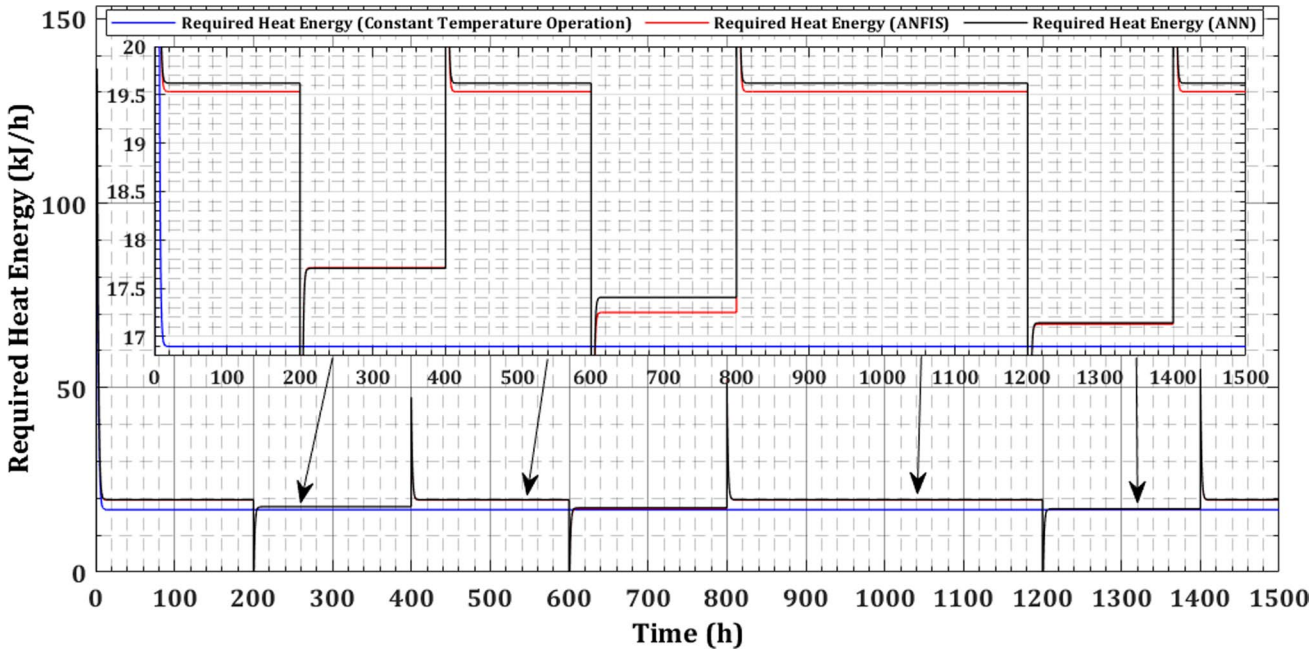

Fig. 25 Graph for variation in required heat energy due to variation in temperature set-point produced from ANFIS and ANN compared with constant temperature operation

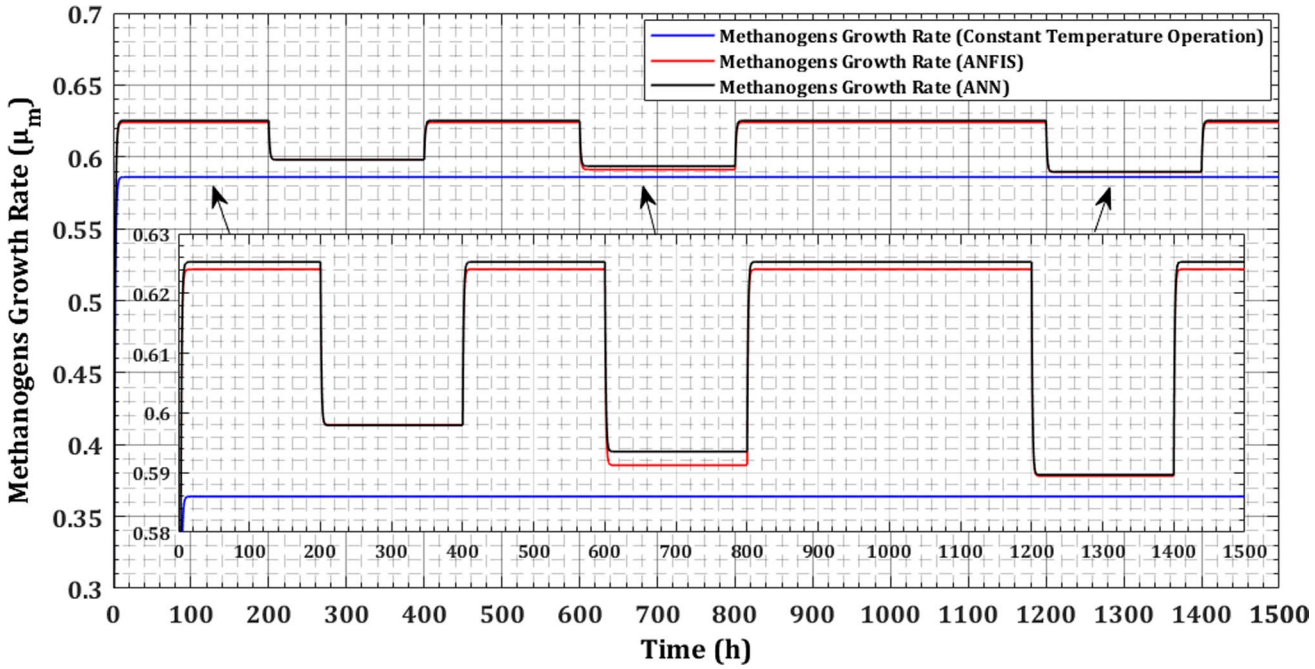

Fig. 26 Graph for variation in the growth rate of methanogens due to variation in temperature set-point produced from ANFIS and ANN compared with constant temperature operation

can be observed that the temperature control has a similar performance to case-1 in this case. ANN has a better rise and settling time compared to ANFIS. In constant temperature operation, the set-point is 55 °C. The flow rate of hot fluid is used to control the temperature of the digester. The flow rate of hot fluid is 0.12305 m^3/h, 0.12303 m^3/h, and 0.12101 m^3/h in the case of ANFIS, ANN, and constant temperature operation, respectively (Fig. 24). The total

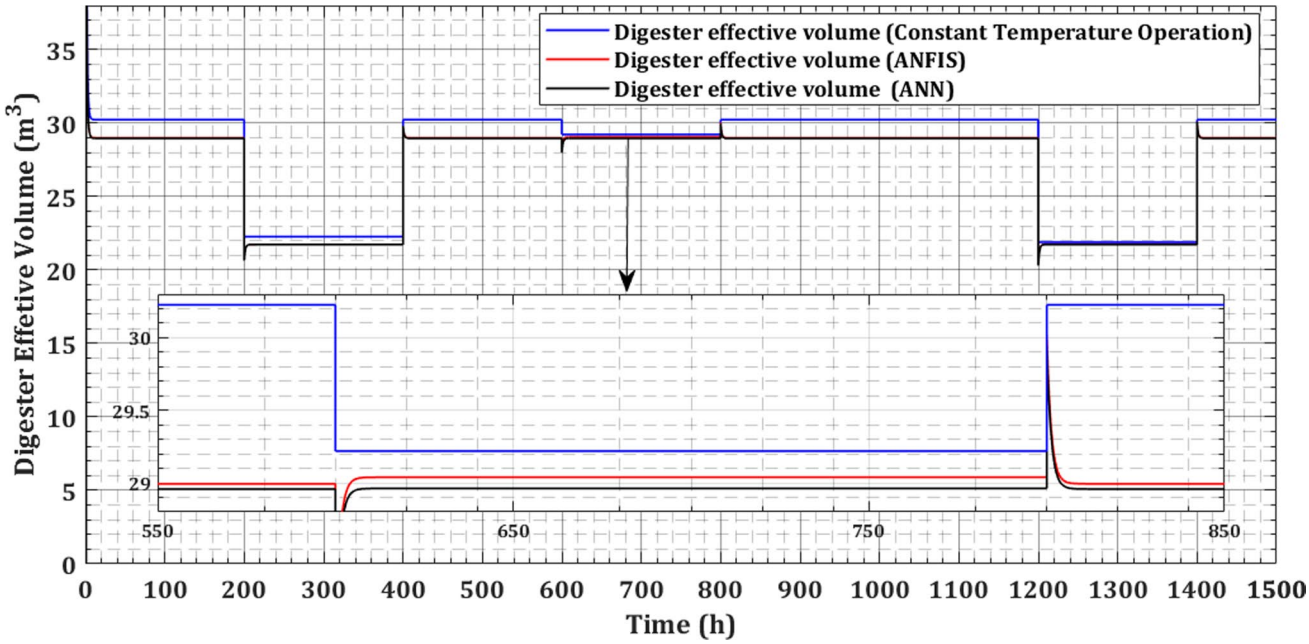

Fig. 27 Graph for variation in digester effective volume due to variation in temperature set-point produced from ANFIS and ANN compared with constant temperature operation

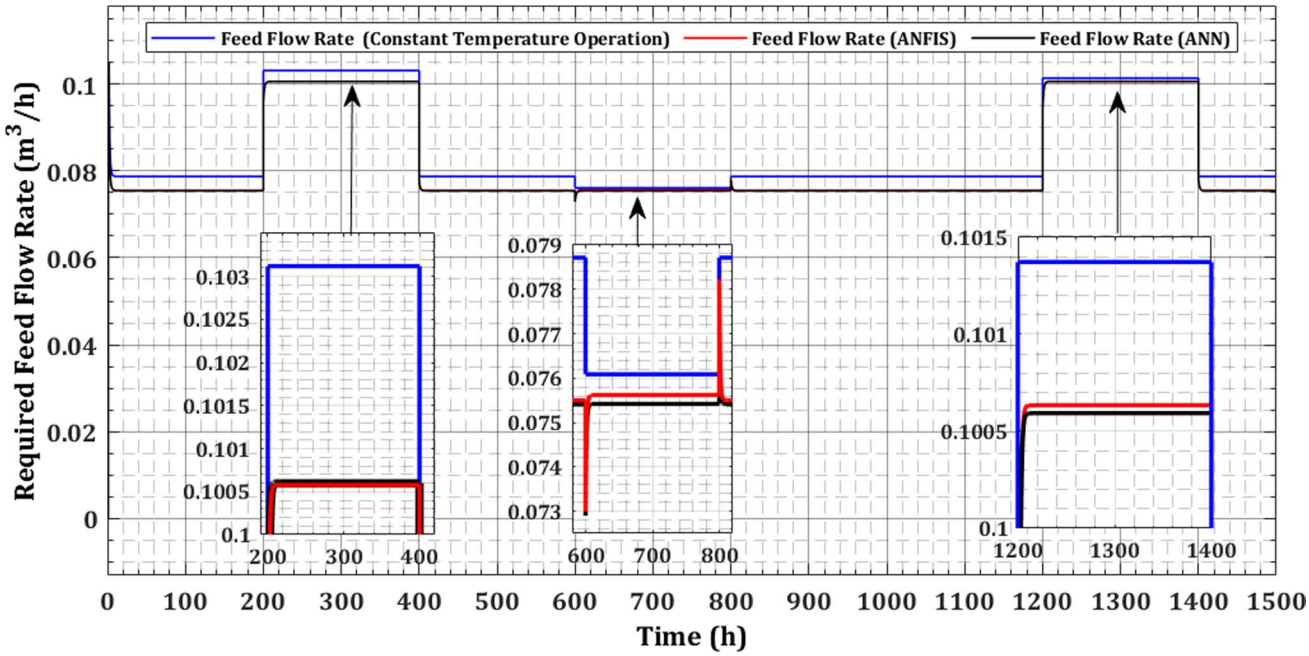

Fig. 28 Graph for variation in required feed flow rate due variation in temperature set-point produced from ANFIS and ANN compared with constant temperature operation

required heat energy to maintain the temperature inside the digester is 17.712 kJ/h, 17.704 kJ/h, and 16.89 kJ/h in the case of ANFIS, ANN, and constant temperature operation, respectively (Fig. 25). The growth rate of methanogens depends on the digester operating temperature. The growth rate of methanogens is 0.598, 0.597, and 0.586 in the case of ANFIS, ANN, and constant temperature operation, respectively (Fig. 26). There is a variation in required digester effective volume due to variation in methane yield because the total volatile solids and hydraulic retention

period are variable. In this case, the required volume of the digester is 21.725 m^3, 21.730 m^3, and 30.22 $6m^3$ in the case of ANFIS, ANN, and constant temperature operation, respectively (Fig. 27). There is a variation in the required feed flow rate due to variation in methane yield because the total volatile solids and hydraulic retention period are variable. In this case, the required volume of the digester is 0.10058 m^3/h, 0.10060 m^3/h, and 0.0787 m^3/h in the case of ANFIS, ANN, and constant temperature operation, respectively (Fig. 28). The obtained methane yield from the digester, in this case, is 2.8999 m^3, $2.8994m^3$, and 2.8284 m^3 in the case of ANFIS, ANN, and constant temperature operation, respectively (Fig. 29). Deviation of methane yield from set-point can be observed in Fig. 30.

Case-3: When VS = 60, B = 4, and required methane yield = 2.9 (600-800 h)

For this case, the temperature set-point determined by ANFIS is 55.402 °C whereas the temperature set-point determined by ANN is 55.579 °C (Fig. 22). From Fig. 23, it can be observed that the system with ANN exhibits the similar

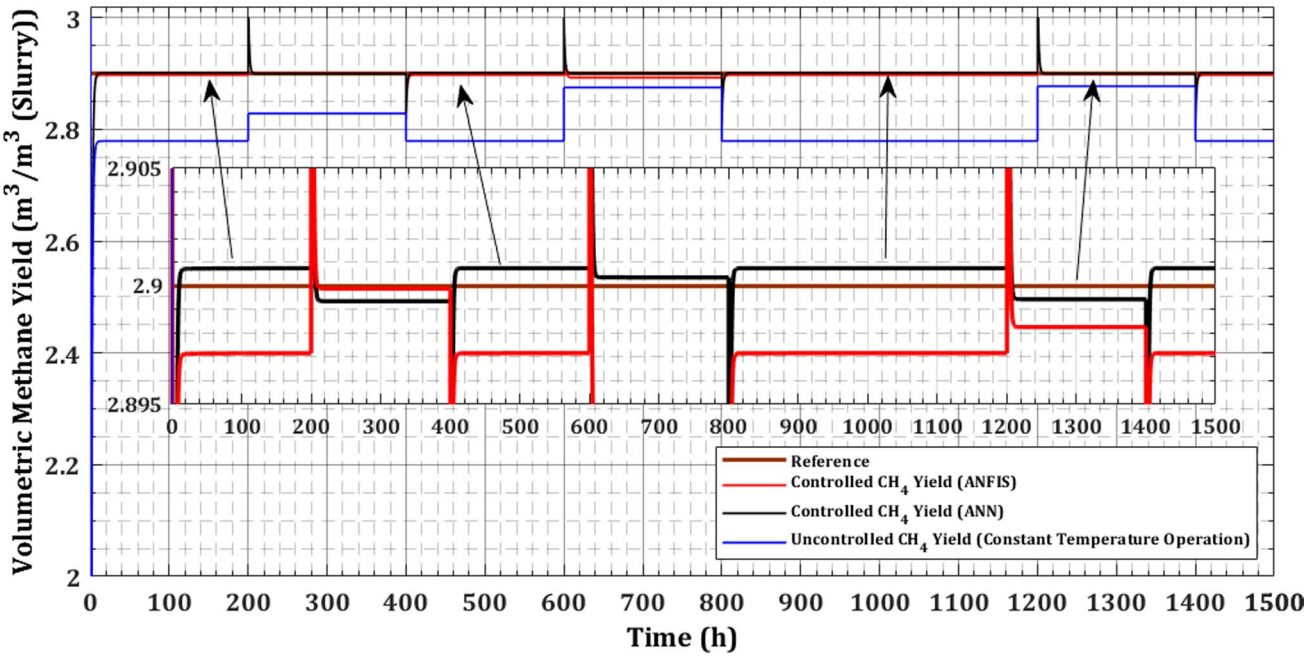

Fig. 29 Graph for variation in volumetric methane yield due to variation in temperature set-point produced from ANFIS and ANN compared with constant temperature operation

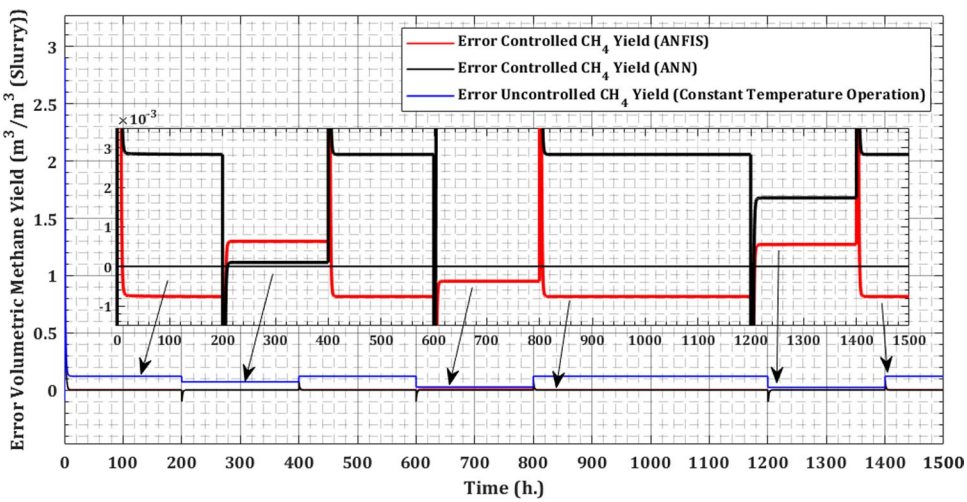

Fig. 30 Graph for variation in error in volumetric methane yield due to variation in temperature set-point produced from ANFIS and ANN compared with constant temperature operation

performance to case-1. In constant temperature operation, the set-point is 55 °C. The flow rate of hot fluid is used to control the temperature of the digester. The flow rate of hot fluid is 0.1219 m^3/h, 0.1223 m^3/h, and 0.1210 m^3/h in the case of ANFIS, ANN, and constant temperature operation, respectively (Fig. 24). The total required heat energy to maintain the temperature inside the digester is 17.25 kJ/h, 17.45 kJ/h, and 16.89 kJ/h in the case of ANN, ANFIS, and constant temperature operation, respectively (Fig. 25). The growth rate of methanogens depends on the digester operating temperature. The growth rate of methanogens is 0.591, 0.594, and 0.586 in the case of ANFIS, ANN, and constant temperature operation, respectively (Fig. 26). There is a variation in required digester effective volume due to variation in methane yield because the total volatile solids and hydraulic retention period are variable. In this case, the required volume of the digester is 29.041 m^3, 29.961 m^3, and 29.218m^3 in the case of ANFIS, ANN, and constant temperature operation, respectively (Fig. 27). There is a variation in the required feed flow rate due to variation in methane yield because the total volatile solids and hydraulic retention period are variable. In this case, the required volume of the digester is 0.0756 m^3/h, 0.0754 m^3/h, and 0.0761 m^3/h in the case of ANFIS, ANN, and constant temperature operation, respectively (Fig. 28). The obtained methane yield from the digester, in this case, is 2.8926 m^3, 2.9004 m^3, and 2.8749 m^3 in the case of ANFIS, ANN, and constant temperature operation, respectively Fig. 29. Deviation of methane yield from set-point can be observed in Fig. 30.

Case-4: When VS = 59, B = 3, and required methane yield = 2.9 (1200-1400 h)

For this case, the temperature set-point determined by ANFIS is 55.26 °C whereas the temperature set-point determined by ANN is 55.28 °C (Fig. 22). From Fig. 23, it can be observed that the system with ANN exhibits the similar performance to case-1. In constant temperature operation, the set-point is 55 °C. The flow rate of hot fluid is used to control the temperature of the digester. The flow rate of hot fluid is 0.1215 m^3/h, 0.1216 m^3/h, and 0.1210 m^3/h in the case of ANFIS, ANN, and constant temperature operation, respectively (Fig. 24). The total required heat energy to maintain the temperature inside the digester is 17.128 kJ/h, 17.142 kJ/h, and 16.89 kJ/h in the case of ANFIS, ANN, and constant temperature operation, respectively (Fig. 25). The growth rate of methanogens depends on the digester operating temperature. The growth rate of methanogens is 0.5894, 0.5896, and 0.586 in the case of ANFIS, ANN, and constant temperature operation, respectively (Fig. 26). There is a variation in required digester effective volume due to variation in methane yield because the total volatile solids and hydraulic retention period are variable. In this case, the required volume of the digester is 21.737 m^3, 21.728 m^3, and 21.899 m^3 in the case of ANFIS, ANN, and constant temperature operation, respectively (Fig. 27). There is a variation in the required feed flow rate due to variation in methane yield because the total volatile solids and hydraulic retention period are variable. In this case, the required volume of the digester is 0.1007 m^3/h, 0.10060 m^3/h, and 0.1014 m^3/h in the case of ANFIS, ANN, and constant temperature operation, respectively (Fig. 28). The obtained methane yield from the digester, in this case, is 2.8982 m^3, 2.8994 m^3, and 2.8772 m^3 in the case of ANFIS, ANN, and constant temperature operation, respectively Fig. 29. Deviation of methane yield from set-point can be observed in Fig. 30.

From the results, it can be observed that the methane yield is closer to the set-point in the inferential control with ANN compared to ANFIS (Figs. 29 and 30). Uncontrolled methane yield is lower compared to inferential control of methane yield with ANFIS and ANN, with the same total volatile solid concentration and hydraulic retention period. The temperature set-point obtained by ANFIS and ANN is higher than 55 °C (constant temperature operation) (Figs. 22 and 23). Due to this, the hot fluid flow rate (Fig. 24) and required heat energy (Fig. 25) are a little bit higher. But the growth rate of methanogens (Fig. 26) is better in the inferential control with ANFIS and ANN. The digester effective volume (Fig. 27) and feed flow rate (Fig. 28) are lower in the inferential control with ANFIS and ANN than in the conventional uncontrolled operation because the digester operating temperature is higher in the inferential control with ANFIS and ANN.

The temperature sensor has been replaced by an equation in the temperature control loop in the proposed control strategy. From the results, it can be observed that the equation is determining the digester temperature accurately (Fig. 23).

4 Conclusion and future scope

In this paper, an inferential control strategy has been proposed to control the methane yield. The desired methane yield is achieved by operating the digester at a temperature value determined based on the concentration of volatile solids and hydraulic retention period by ANFIS and ANN, for a stable heat and power generation. From the results, it is evident that the proposed inferential control strategy is effectively controlling the methane yield. The performance of ANN is better compared to ANFIS. The temperature control

with the PIDF controller tuned with the BF-PSO optimization algorithm is working efficiently. Temperature control without a temperature sensor is performing very similar to temperature control with a temperature sensor. The heat energy requirement varies according to the digester operating temperature. The proposed strategy increases and stabilizes the methane yield. Furthermore, it allows the operator to achieve the desired level of methane yield. The proposed strategy makes the AD plant more energy efficient. The proposed control strategy was simulated in MATLAB/Simulink 2021a environment. However, exploring the exergy with the proposed strategy will be interesting.

Author contribution Kundan Anand: conceptualization, methodology, software, formal analysis, investigation, resources, data curation, writing – original draft, and visualization. Alok Prakash Mittal: conceptualization and supervision. Bhavnesh Kumar: conceptualization, validation, writing – review and editing, and supervision.

Declarations

Conflict of interest The authors declare no competing interests.

References

1. Ke T, Yun S, Wang K et al (2022) Enhanced anaerobic co-digestion performance by using surface-annealed titanium spheres at different atmospheres. Bioresour Technol 347:126341. https://doi.org/10.1016/j.biortech.2021.126341
2. Wang K, Yun S, Ke T et al (2022) Use of bag-filter gas dust in anaerobic digestion of cattle manure for boosting the methane yield and digestate utilization. Bioresour Technol 348:126729. https://doi.org/10.1016/j.biortech.2022.126729
3. Tabatabaei M, Aghbashlo M, Valijanian E et al (2020) A comprehensive review on recent biological innovations to improve biogas production. Part 1: Upstream strategies. Renew Energy 146. https://doi.org/10.1016/j.renene.2019.07.037
4. Han F, Yun S, Zhang C et al (2019) Steel slag as accelerant in anaerobic digestion for nonhazardous treatment and digestate fertilizer utilization. Bioresour Technol 282:331–338. https://doi.org/10.1016/J.BIORTECH.2019.03.029
5. Li B, Yun S, Xing T et al (2021) A strategy for understanding the enhanced anaerobic co-digestion via dual-heteroatom doped biobased carbon and its functional groups. Chem Eng J 425. https://doi.org/10.1016/j.cej.2021.130473.
6. Nsair A, Onen Cinar S, Alassali A et al (2020) Operational parameters of biogas plants: a review and evaluation study. Energies 13:3761. https://doi.org/10.3390/en13153761
7. Al-Addous M, Alnaief M, Class C et al (2017) Technical possibilities of biogas production from olive and date waste in Jordan. BioResources. https://doi.org/10.15376/biores.12.4.9383-9395
8. Pachauri N, Singh V, Rani A (2017) Two degree of freedom PID based inferential control of continuous bioreactor for ethanol production. ISA Trans 68:235–250. https://doi.org/10.1016/j.isatra.2017.03.014
9. Abbas Y, Yun S, Wang K et al (2021) Static-magnetic-field coupled with fly-ash accelerant: a powerful strategy to significantly enhance the mesophilic anaerobic-co-digestion. Bioresour Technol 327. https://doi.org/10.1016/j.biortech.2021.124793
10. Yun S, Xing T, Han F et al (2021) Enhanced direct interspecies electron transfer with transition metal oxide accelerants in anaerobic digestion. Bioresour Technol 320. https://doi.org/10.1016/j.biortech.2020.124294
11. Smith CA (2002) Automated continuous process control. John Wiley & Sons Inc, New York, USA
12. Chéruy A (1997) Software sensors in bioprocess engineering. J Biotechnol 52:193–199. https://doi.org/10.1016/S0168-1656(96)01644-6
13. Najafi B, Faizollahzadeh Ardabili S (2018) Application of ANFIS, ANN, and logistic methods in estimating biogas production from spent mushroom compost (SMC). Resour Conserv Recycl 133:169–178. https://doi.org/10.1016/j.resconrec.2018.02.025
14. Zareei S, Khodaei J (2017) Modeling and optimization of biogas production from cow manure and maize straw using an adaptive neuro-fuzzy inference system. Renew Energy 114:423–427. https://doi.org/10.1016/j.renene.2017.07.050
15. Okwu MO, Samuel OD, Ewim DRE, Huan Z (2021) Estimation of biogas yields produced from combination of waste by implementing response surface methodology (RSM) and adaptive neuro-fuzzy inference system (ANFIS). Int J Energy Environ Eng. https://doi.org/10.1007/s40095-021-00381-5
16. Arumugam T, Parthiban L, Rangasamy P (2015) Two-phase anaerobic digestion model of a tannery solid waste: experimental investigation and modeling with ANFIS. Arab J Sci Eng 40:279–288. https://doi.org/10.1007/s13369-014-1408-9
17. Okwu MO, Samuel OD, Otanocha OB et al (2020) Development of ternary models for prediction of biogas yield in a novel modular biodigester: a case of fuzzy Mamdani model (FMM), artificial neural network (ANN), and response surface methodology (RSM). Biomass Convers Biorefinery. https://doi.org/10.1007/s13399-020-01113-1
18. Yousefi-Darani A, Paquet-Durand O, Hinrichs J, Hitzmann B (2021) Parameter and state estimation of backers yeast cultivation with a gas sensor array and unscented Kalman filter. Eng Life Sci 21:170–180. https://doi.org/10.1002/elsc.202000058
19. Samuel OD, Okwu MO, Tartibu LK et al (2021) Modelling of *Nicotiana tabacum* L. oil biodiesel production: Comparison of ANN and ANFIS. Front Energy Res 8. https://doi.org/10.3389/fenrg.2020.612165
20. Elumalai PV, Krishna Moorthy R, Parthasarathy M et al (2022) Artificial neural networks model for predicting the behavior of different injection pressure characteristics powered by blend of biofuel-nano emulsion. Energy Sci Eng. https://doi.org/10.1002/ese3.1144
21. Samuel OD, Kaveh M, Oyejide OJ et al (2022) Performance comparison of empirical model and Particle Swarm Optimization & its boiling point prediction models for waste sunflower oil biodiesel. Case Stud Therm Eng 33. https://doi.org/10.1016/j.csite.2022.101947
22. Li XM, Chen XD, Chen LZ, Nguang SK (2004) Soft sensors for on-line biomass measurements. Bioprocess Biosyst Eng 26:191–195. https://doi.org/10.1007/s00449-004-0350-8
23. Wang Z, Yun S, Xu H, et al (2019) Mesophilic anaerobic co-digestion of acorn slag waste with dairy manure in a batch digester: focusing on mixing ratios and bio-based carbon accelerants. Bioresour Technol 286. https://doi.org/10.1016/j.biortech.2019.121394
24. Nguyen D, Gadhamshetty V, Nitayavardhana S, Khanal SK (2015) Automatic process control in anaerobic digestion technology: a critical review. Bioresour Technol 193:513–522. https://doi.org/10.1016/j.biortech.2015.06.080

25. Chen YR, Varel VH, Hashimoto AG (1980) Effect of temperature on methane fermentation kinetics of beef-cattle manure. United States
26. Su B, Han W, Zhang X et al (2018) Assessment of a combined cooling, heating and power system by synthetic use of biogas and solar energy. Appl Energy 229:922–935. https://doi.org/10.1016/j.apenergy.2018.08.037
27. Zhang G, Li Y, Dai YJ, Wang RZ (2016) Design and analysis of a biogas production system utilizing residual energy for a hybrid CSP and biogas power plant. Appl Therm Eng 109:423–431. https://doi.org/10.1016/j.applthermaleng.2016.08.092
28. Saeed M, Fawzy S, El-Saadawi M (2019) Modeling and simulation of biogas-fueled power system. Int J Green Energy 16:125–151. https://doi.org/10.1080/15435075.2018.1549997
29. Karaboga D, Kaya E (2019) Adaptive network based fuzzy inference system (ANFIS) training approaches: a comprehensive survey. Artif Intell Rev 52:2263–2293. https://doi.org/10.1007/s10462-017-9610-2
30. Walia N, Singh H, Sharma A (2015) ANFIS: Adaptive Neuro-Fuzzy Inference System- A Survey. Int J Comput Appl 123:32–38. https://doi.org/10.5120/ijca2015905635
31. Tan Y, Shuai C, Jiao L, Shen L (2017) An adaptive neuro-fuzzy inference system (ANFIS) approach for measuring country sustainability performance. Environ Impact Assess Rev 65:29–40. https://doi.org/10.1016/j.eiar.2017.04.004
32. Okwu MO, Tartibu LK, Samuel OD et al (2021) Predictive ability of Response Surface Methodology (RSM) and Artificial Neural Network (ANN) to approximate biogas yield in a modular biodigester. In: Lecture Notes in Computer Science (including subseries Lecture Notes in Artificial Intelligence and Lecture Notes in Bioinformatics), pp 202–215. https://doi.org/10.1007/978-3-030-85030-2_17
33. Kazemi P, Steyer J-P, Bengoa C et al (2020) Robust data-driven soft sensors for online monitoring of volatile fatty acids in anaerobic digestion processes. Processes 8:67. https://doi.org/10.3390/pr8010067
34. Sheela KG, Deepa SN (2013) Review on methods to fix number of hidden neurons in neural networks. Math Probl Eng 2013:1–11. https://doi.org/10.1155/2013/425740
35. Thomas AJ, Petridis M, Walters SD et al (2015) On predicting the optimal number of hidden nodes. In: 2015 International Conference on Computational Science and Computational Intelligence (CSCI), IEEE, pp 565–570. https://doi.org/10.1109/CSCI.2015.33
36. Ogunbo JN, Alagbe OA, Oladapo MI, Shin C (2020) N-hidden layer artificial neural network architecture computer code: geophysical application example. Heliyon 6:e04108. https://doi.org/10.1016/j.heliyon.2020.e04108
37. Almabrok A, Psarakis M, Dounis A (2018) Fast tuning of the PID controller in an HVAC system using the Big Bang-Big Crunch algorithm and FPGA technology. Algorithms 11. https://doi.org/10.3390/a11100146
38. Jahanshahi E, De Oliveira V, Grimholt C, Skogestad S (2014) A comparison between internal model control, optimal PIDF and robust controllers for unstable flow in risers. IFAC Proc 47:5752–5759. https://doi.org/10.3182/20140824-6-ZA-1003.02381
39. Manik S (2020) Control system model reduction using hybrid optimization approach. Int J Adv Trends Comput Sci Eng 9:4006–4011. https://doi.org/10.30534/ijatcse/2020/225932020
40. Korani WM, Dorrah HT, Emara HM (2009) Bacterial foraging oriented by Particle Swarm Optimization strategy for PID tuning. In: 2009 IEEE International Symposium on Computational Intelligence in Robotics and Automation - (CIRA). IEEE, pp 445–450. https://doi.org/10.1109/CIRA.2009.5423165
41. Anand K, Mittal AP, Kumar B (2021) Modelling and simulation of dual heating of substrate with centralized temperature control for anaerobic digestion process. J Clean Prod 325:129235. https://doi.org/10.1016/j.jclepro.2021.129235